ICES Journal of Marine Science, 2024, Vol. 0, Issue 0, 1–18
https://doi.org/10.1093/icesjms/fsae147
Received: 3 June 2024; **revised:** 25 September 2024; **accepted:** 7 October 2024
Original Article

Latitudinal gradients in zooplankton communities in Norwegian fjords resolved by an integrated morphological and molecular approach

Elizaveta A. Ershova*, Terje Berge, Gastón E. Aguirre, Magnus J. Reeve, Monica B. Martinussen, Tone Falkenhaug

Institute of Marine Research, P.O. Box 1870, Nordnes, Bergen NO-5817, Norway
*Corresponding author. Institute of Marine Research, P.O. Box 1870, Nordnes, Bergen NO-5817, Norway. E-mail: elizaveta.ershova@hi.no

Abstract

Fjords are coastal habitats that are often partially isolated from surrounding shelf waters and can contain ecologically unique and diverse ecosystems. Here, we offer a comprehensive overview of zooplankton communities at the end of the productive season across 34 fjord locations along the Norwegian west coast, ranging from 62 to 69°N latitude. We applied an integrated methodological approach that included traditional microscopy, FlowCam image analysis, community DNA metabarcoding, and bulk size-fractionated biomass measurements. Together, these combined data revealed distinct geographical patterns in zooplankton quantity and community composition. Water temperature, which was closely correlated to latitude, and bottom depth were the most important physical parameters driving zooplankton biomass, abundance, community structure, and size distribution. Multivariate analysis of species composition using both microscopy and metabarcoding-derived data identified three distinct assemblages that were strongly correlated to temperature, latitude, and bottom depth. Our comparison of the applied methodologies demonstrated differential strengths and limitations of these methods as monitoring tools for capturing zooplankton community dynamics. Our study underscores the need for continued, multifaceted biological surveys that can help inform effective ecosystem management and conservation strategies in response to climate-related and anthropogenic pressures.

Keywords: zooplankton; pelagic ecosystems; coastal ecosystems; FlowCAM; metabarcoding

Introduction

Norwegian fjords are unique coastal environments that were carved by glaciers during the last ice age and subsequently flooded by rising sea levels when the glaciers retreated. They can be much deeper than the surrounding continental shelf (>500 m) and extend far inland, creating a complex array of marine habitats due to their steep bathymetric gradients, ranging from shallow intertidal zones to deep basins (Inall and Gillibrand 2010). Typically, a shallow sill is present either at the entrance of the fjord or as a shallow coastal plateau just outside the fjord, restricting exchange of water between the fjord and the open ocean and influencing circulation patterns. Consequently, fjords can often harbor ecosystems that are partially isolated from adjacent coastal and offshore environments, often resulting in very different production and diversity patterns (Skjøldal et al. 1995). The Norwegian west coast has the highest concentration of fjords in the world, with the total number of fjords estimated to be over 1000. Beyond their ecological importance, fjords significantly impact Norway's socioeconomic structure, supporting fisheries, aquaculture, tourism, and serving as conduits for maritime transport. The high biological productivity of fjords is central to local and national fishing industries, providing spawning and nursery grounds for many commercial fish species. Fish farming is also heavily dependent on the health and function of fjord systems (Skaala et al. 2014). Many fjords also attract a substantial number of tourists, which supports local economies and highlights their cultural and recreational value. These increased anthropogenic pressures, however, come with environmental challenges such as habitat disturbance, pollution, and the introduction of invasive species (Weatherdon et al. 2016). This drives a need for comprehensive ecological assessments that will allow to dictate sustainable practices.

Zooplankton are integral components of marine ecosystems, serving as primary consumers of algal and microbial production and as primary prey for various fish species of commercial importance (Steinberg and Landry 2017). Given their rapid response to environmental alterations, changes in zooplankton communities can reflect broader ecosystem shifts (Richardson 2008, Ratnarajah et al. 2023). Such shifts, e.g. geographical range expansions or contractions due to climate change, or the appearance of invasive species, can have profound implications for nutrient cycling, food web dynamics, and overall ecosystem resilience (Renaud et al. 2018, Weydmann et al. 2018, Polyakov et al. 2020). Monitoring zooplankton can not only reflect immediate ecological shifts in the zooplankton communities, but may also anticipate potential cascading effects on higher trophic levels that can impact commercial fisheries and biodiversity. Pelagic communities in fjords are composed of a mixture of organisms that maintain local populations there, as well as advected organisms from adjacent shelf regions (Aksnes et al. 1989). The relative isolation of most sill fjords makes them ideal natural

laboratories for examining how local environmental factors can drive community composition and distribution patterns, while more open fjords can reflect broader oceanographic patterns in the coastal areas.

Pelagic communities have been described in detail for many individual fjords, both as single-season studies and over longer periods (Hopkins 1981, Hopkins et al. 1984, Falkenhaug et al. 1997, Michelsen et al. 2017, Coguiec et al. 2021). There have also been several works that compare several fjords in the same region (Somme 1934, Strømgren 1975, Gorsky et al. 2000). Yet there is a notable lack of comprehensive studies investigating zooplankton communities across multiple fjords, particularly over a significant latitudinal range. This broader approach is essential for understanding regional biodiversity patterns and ecological variability across larger spatial scales. This study addresses this gap by investigating zooplankton communities within 21 fjords along the west coast of Norway, spanning from Balsfjord at ~70°N, to Vanylvsfjorden at 62°N. We utilize an integrated methodological approach that included traditional microscopy (taxonomy and counts), FlowCam image analysis, community DNA metabarcoding, and size-fractionated biomass assessments of net-collected samples to generate a multi-dimensional perspective on zooplankton communities. Additionally, we include a critical comparison of the employed methodologies, assessing their strengths and limitations as monitoring tools for capturing zooplankton community dynamics.

While this study is based on a single, opportunistic survey, and thus represents a snapshot within one seasonal cycle, it helps establish a foundational baseline for zooplankton monitoring and research in Norwegian fjord systems. Given the dynamic and sensitive nature of fjord ecosystems, our study underscores the need for continued, large-scale biological surveys to inform effective ecosystem management and conservation strategies in response to climate-related and anthropogenic pressures.

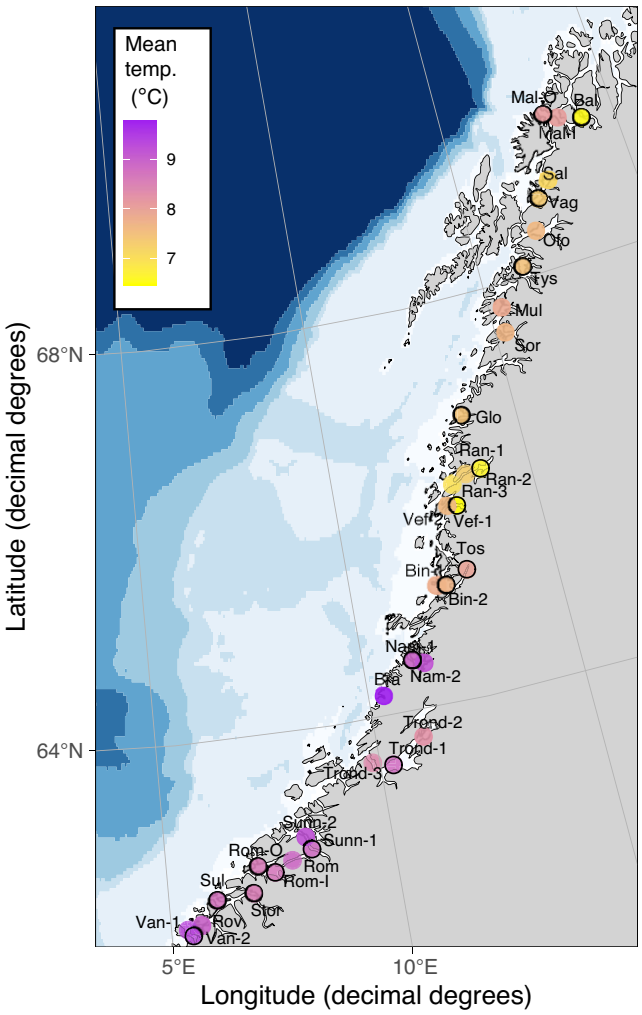

Figure 1. Sampling locations and mean water temperature. Circles with a solid black border indicate stations where ethanol samples were taken and the formalin samples were analyzed microscopically.

Methods

Sampling

Sampling was conducted in 34 fjord locations (Fig. 1) onboard R/V Kristine Bonnevie from 13 October to 8 November 2021. Temperature, salinity, and fluorescence in the water column were measured using a Sea-Bird SBE 9 CTD lowered to 10 m above the seafloor. Zooplankton was collected using a WP-II net (0.25 m^2 diameter mouth opening, 180 μm mesh size), hauled vertically from 5 m off the sea floor to the surface. At stations deeper than 200 m, a second net tow was taken from 200 m to the surface. There was no observable clogging of the nets. The whole sample was immediately scanned for large (>2 cm) gelatinous organisms (scyphozoan jellyfish and ctenophores). The total abundance and volume (ml) of each gelatinous group was measured, after which they were discarded. The remainder of the sample was split using a Motoda splitter (Motoda 1959) for taxonomic analysis and biomass measurements. Half of the sample was sieved through a series of mesh sizes (2000, 1000, and 180 μm); the sample from each sieve then rinsed with freshwater and transferred onto pre-weighed aluminum trays. The 2000 μm (macrozooplankton) fraction was further separated into taxonomic groups prior to being placed on pre-weighed trays, with one tray per group. The trays were dried at 65°C for 24 h, then frozen at −20°C. At 17 stations, the remaining half of the sample was split one more time, and half of the split (1/4 of the original sample) was preserved in 4% borax-buffered formaldehyde-seawater solution, while the other 1/4 was preserved in 100% ethanol (Fig. 1). At the remaining stations, the whole ½ split was preserved in formaldehyde.

Biomass estimation

In the lab, the aluminum trays containing the size-fractionated dry weight samples were heated to 65°C once more for 6 h to remove traces of moisture from the freezer, then weighed on a Sartorius Quintix 224-1CEU scale (precision = 0.1 mg). For stations deeper than 200 m where 2 net tows were taken, the biomass of the 200 m tow was subtracted from the full water column tow to get the biomass of zooplankton below 200 m. The volume of water filtered by the plankton net was estimated by multiplying the mouth area by the towing distance (depth of deployment).

Microscopy

The formalin preserved samples were taxonomically enumerated via microscopy at 16 of the stations where ethanol preserved samples were taken. Large individuals (>2000 μm)

were counted in the whole sample, while smaller and more numerous taxa were counted in sub-samples of 1/2 to 1/128, which were obtained using a Motoda splitter. A total of 200–1000 individuals were typically counted in each sample. Copepods were identified to species or genus level (*Pseudocalanus* spp. and *Paracalanus parvus* were grouped as *Pseudo-/Paracalanus* spp.), but for most other groups classification was assigned as broad taxonomic categories. Copepodite stages were determined for *Calanus* spp., *Paraeuchaeta* spp., *Pseudo-/Paracalanus* spp., and *Metridia* spp., while other copepod species were counted as adults/copepodites. The two sibling species *Calanus finmarchicus* and. *Calanus helgolandicus* were distinguished by the characters of the fifth legs according to Fleminger and Hulsemann (1977). For each sample, 20 individuals of *Calanus* stage C5, adult females, and adult males were identified by species, and the proportions within each stage were used to calculate the total number in the sample. Copepodite stages C1–C4 were counted but for these stages the two species cannot be separated morphologically.

FlowCam image analysis

The 16 formalin preserved samples were also imaged using a FlowCam macro (Yokogawa Fluid Imaging Technologies, USA) and classified using supervised machine learning. The organisms were filtered onto a 180 µm mesh and diluted in 2.75 l of freshwater to avoid the presence of multiple organisms in the same image. An overhead stirrer kept the zooplankton organisms in suspension, and ca. 70% of the sample was imaged, resulting in 2000–50 000 images per sample. Due to the cameras field of view, flowcell dimensions, sample flowrate, and camera frame rate ca. 30% of the sample was not imaged to avoid multiple images the same particle/sample. The FlowCam was fitted with a 5 × 5 mm flowcell and a 0.5X objective, and the instrument software VisualSpreadsheet© 4.12.3 was used during the imaging. A size filter based on Area-Based-Diameter was set to 150–3000 µm. The context settings of the FlowCam analyses are found in Supplementary Material 1.

DNA Metabarcoding

Ethanol was removed from the samples and replaced with MilliQ water. The samples were homogenized for 2 × 30 s using a mixture of 2 and 5 mm ceramic beads on the 2 × 150 Precellys bead-beating machine. Three 300 μl replicates of the resulting homogenate were extracted using the Qiagen Blood and Tissue Kit via the manufacturer's protocol. The PCR and library prep protocols, as well as the bioinformatics pipeline, were identical to those described in Ershova et al. (2023). Final species assignments of the resulting MOTU's (molecular operational taxonomic units) were made using the Python-based application BOLDigger (Buchner and Leese 2020). A species level assignment was typically made at 98% similarity; the following thresholds were applied for non-species level matches: 95%—genus, 90%—family, 85%—order, <85%—class). An exception was the species *Parasagitta elegans*, which was assigned at a 90% similarity level due to the extremely high intraspecies variation of the COI gene in this group (Marlétaz et al. 2017). MOTU's with ambiguous assignments (more than one species level match) or non-species level assignments were flagged and verified individually on a case-to-case basis, as discussed in Ershova et al. (2023). The three extraction replicates were pooled for analysis. Species-level identifications were assigned a biogeographic affinity based on their distribution ranges in the North Atlantic as documented on the World Register of Marine Species (Ahyong et al. 2024). Four biogeographic categories were assigned: *Arctic/Arctoboreal* (primary distribution range above 65°N); *Boreal* (primary distribution range between 55–65°N), *Temperate* (primary distribution range below 55°N), and *Cosmopolitan* (cosmopolitan distribution range).

Data analysis

All analyses were carried out in R version 4.1.2 (R Core Team 2022). Maps and species distributions were plotted using the ggOceanMaps package (Vihtakari 2024). Temperature, salinity and flourescence data were binned for every 1 m, and mean values were obtained for surface (0–10 m), bottom (20–10 m above the seafloor), and mean (whole water column) layers. Zooplankton biomass was expressed as g m^{-3} by dividing with estimated filtered volume to facilitate comparability of plankton densities between stations of varying depths.

The raw images from the FlowCam were cut into individual particle jpg files, and features were extracted using the r-package fc2zi (described in Álvarez et al. 2012, but modified in 2020 for the flowcam Macro). To make a machine learning classifier, we used the r-package zooimage (Grosjean et al. 2018). Supervised learning involved annotation of 23 200 images by specialist taxonomists into 16 zooplankton groups and one non-plankton (including fibers, bubbles, debris, and background images). A random forest classification model was trained on the annotated dataset and had an overall error rate of 11.1% (determined by 10-fold cross validation). A few groups had higher error rate (maximum 26%). The classifier statistics, including the confusion matrix, can be found in Supplementary Material 2. Based on the results of the automatic classification of the image data, abundances and biovolumes were estimated for each of the plankton groups. To derive plankton size spectra parameters, the FlowCam estimated abundances and biovolumes were distributed into size classes and normalized by the width of the size-class (Álvarez et al. 2014), resulting in normalized abundance size spectra (NASS) and normalized biovolume size spectra (NBSS). The lower range in the size-class was used to describe the width, and each consecutive size-class was twice as large as the previous one in terms of biovolume (mm^3). Slopes and intercepts of the $\log_{10}$–$\log_{10}$ regression lines of normalized abundance and biovolume as a function og organism size (mm^3) were calculated per sample.

Within the metabarcoding dataset, the sequence counts were rarified to the minimum number of per-sample reads using the GUniFrac package (Chen and Chen 2018). Resulting sequence counts were converted to a semi-quantitative metric called biomass-weighed sequence reads (BWSR; Ershova et al. 2023) by multiplying the proportion of sequence reads of each species by total sample biomass as estimated from the dry weight measurements. Trends between total and size-fractionated biomass, microscopy-derived abundance, and normalized biomass size spectra (NBSS) and physical parameters (latitude, temperature, salinity, sill depth, and mean Chl-a) were investigated using generalized additive models (GAMs) fitted with a Tweedie distribution using the mgcv package

Table 1. Station locations and characteristics of sampled fjords. Samples with taxonomic analysis were done microscopically, via FlowCAM and metabarcoding; the remainder only include size-fractionated dry weight data.

Stn.	Lat.	Long.	Fjord name	Abbrev.	Length (km)	Max width (km)	Orientation	Sill depth (m)	Dist. to sill (km)	Max fjord depth (m)	Sampl. depth (m)	Taxon. analysis
1064	69.39	19.04	Balsfjord	Bal	50	5	SE	35	25	195	187	x
1068	69.46	18.38	Malangen (inner)	Mal-I	50	6	SE	210	33	450	230	
1072	69.54	18.01	Malangen (outer)	Mal-O	50	6	SE	210	15	450	380	x
1077	68.89	17.58	Salangen	Sal	18	4	NE	35	5	325	315	
1080	68.74	17.16	Vagsfjorden	Vag	50	10	SE	240	50	500	302	x
1081	68.43	16.82	Ofotfjorden	Ofo	65	13	E	200	29	510	500	
1083	68.12	16.19	Tysfjorden	Tys	45	4.5	S	205	22	725	708	x
1087	67.78	15.35	Nordfolda	Mul	30	7	NE	225	19	290	280	
1090	67.52	15.27	Sorfolda	Sor	40	3.5	SE	265	11	573	550	
1101	66.82	13.62	Glomfjorden	Glo	25	4	E	100	15	375	370	x
1106	66.25	13.77	Ranfjorden	Ran-1	65	5	NE	100	41	530	528	x
1107	66.23	13.37	Ranfjorden	Ran-2	65	5	NE	100	24	530	290	
1108	66.16	12.99	Ranfjorden	Ran-3	65	5	NE	100	7	530	435	
1109	65.94	12.98	Vefsnfjorden	Vef-1	51	4	NE	85	32	483	482	x
1111	65.96	12.75	Vefsnfjorden	Vef-2	51	4	NE	86	21	483	210	
1114	65.19	12.07	Bindals-fjorden	Bin-1	71	3.5	NE	200	3	741	1114	
1115	65.18	12.30	Bindals-fjorden	Bin-2	71	3.5	NE	200	18	741	733	x
1116	65.29	12.87	Tosenfjorden	Tos	39	2.5	NE	200	54	553	419	x
1119	64.51	11.16	Namsen-fjorden	Nam-1	35	5	SE	250	15	454	384	x
1120	64.46	11.42	Namsen-fjorden	Nam-2	35	5	SE	200	25	454	265	
1122	64.21	10.36	Brandsfjorden	Bra	10	2	SE	77	2	143	125	
1126	63.51	10.29	Trondheims-fjorden	Trond	130	20	NE	200	40	617	476	x
1129	63.73	11.07	Trondheims-fjorden	Trond-2	130	20	NE	200	72	617	410	
1131	63.57	9.84	Trondheims-fjorden	Trond-3	130	20	NE	200	5	617	540	
1134	62.81	8.21	Tingvoll-fjorden	Ting	52	3	SE	130	32	365	323	x
1138	62.71	6.99	Romsdal-fjorden (outer)	RomO	88	9	E	180	5	550	481	x
1140	62.63	7.35	Romsdal-fjorden (inner)	RomI	88	9	E	180	27	550	421	x
1145	62.42	6.04	Sulafjorden	Sul	9	5	SE	120	8	445	445	x
1146	62.45	6.83	Storfjorden	Stor	110	4	SE	120	52	679	671	x
1150	62.09	5.46	Vanylvs-fjorden	Van	30	4	SE	100	20	252	240	x

in R, which automatically calculates the dispersion parameter of the model (Wood 2011). Forward stepwise selection was used the choose the best model, with the AIC (Akaike Selection Criterion) used as a selection criterion (Akaike 1974). The fit of the dispersion statistics, spatial independence, and heterodescacity of the models were validated by plotting the residuals against the fitted values, the covariates, and spatial coordinates. Relationships between BWSR and abundance, and between BWSR and macroplankton biomass were described using simple linear regression. Values were square-root transformed to meet the assumption of equal variance.

Community structure was investigated using non-metric multidimensional scaling (nMDS) using the package vegan (Oksanen et al. 2016). The ordination was carried out on Bray–Curtis dissimilarities of square-root transformed microscopy-derived species abundances and square-root transformed species BWSR. The species/taxa responsible for driving the ordination, as well as the environmental parameters significantly correlated with the ordination axes, were identified via the function *envfit* at a significance level of $P = .05$ and visualized as biplots.

Results

Environmental conditions

The sampled fjords ranged from 30 to 150 km in length, with a maximum width between 3 and 20 km. The fjords had pronounced sills that ranged in depth from 35 to 265 m, and a maximum basin depth of 200-700 m (Table 1). Balsfjord (Bal) at the northernmost location was the shallowest of the sampled fjords, and Storfjorden (Stor) and Bindalsfjorden (Bin)—the deepest. Physical properties of the water column followed a similar general pattern, characteristic of Norwegian fjords in autumn (Skjøldal et al. 1995) (Fig. 2, Supplementary Material 3), with a mixed layer depth of 100–120 m, with the upper layer containing Surface water ($S < 34$) and deeper layers containing Norwegian Coastal Water (NwCW) ($S = 32$–35) and Norwegian Atlantic Water (NwAW) ($S > 35$). In some fjords a distinct freshwater lens was present at the surface, with surface salinity as low as 15–20. This was most pronounced in the mid-latitude fjords (Ran, Vef, Tos, Nam). Water temperature reached its maximum around 80–100 m, where it was typically around 10°C–12°C. Underlying this maximum was a sharp pycnocline,

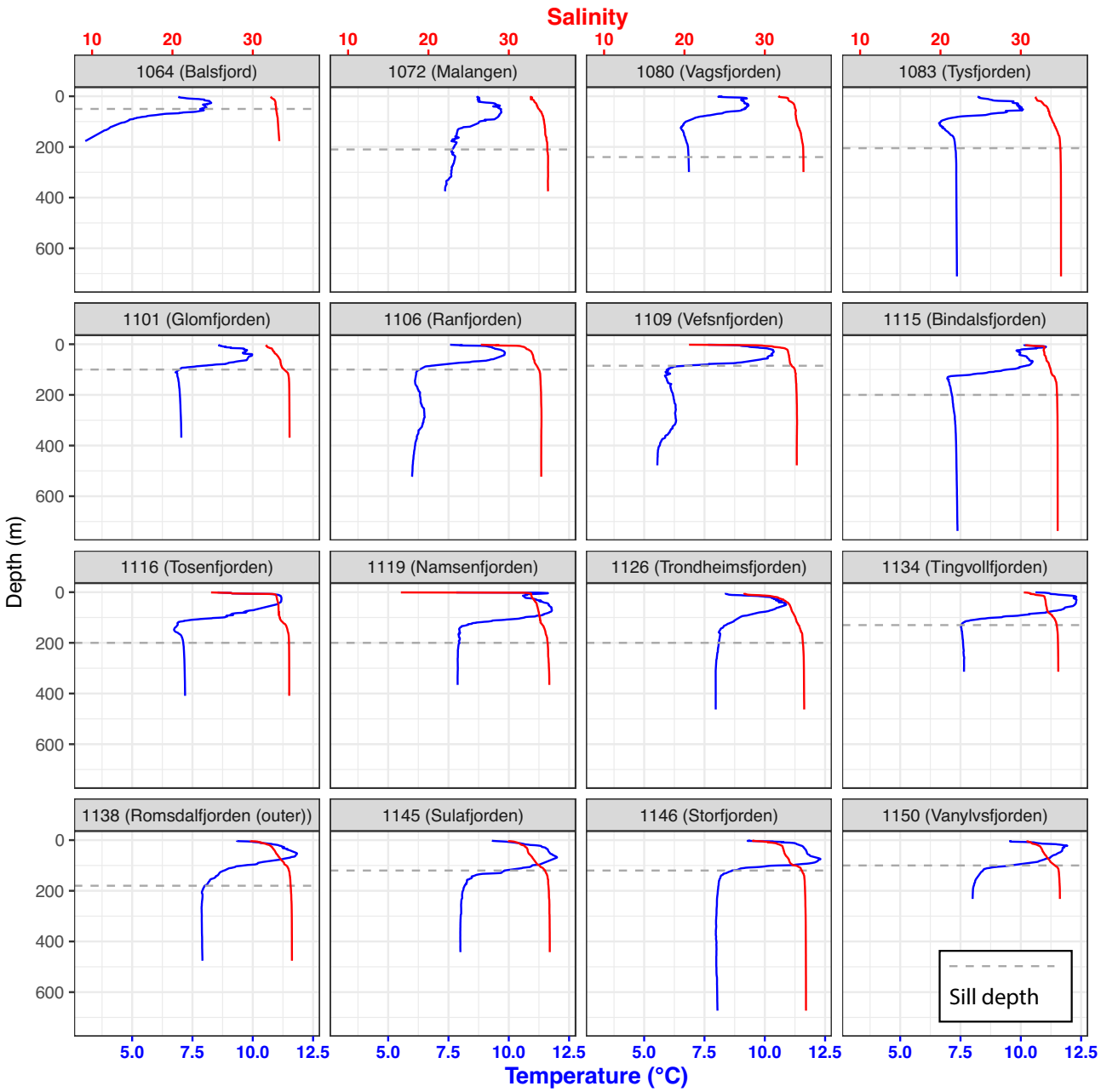

Figure 2. Water column properties (temperature, salinity, and sill depth) of examined stations (only stations where zooplankton samples were examined taxonomically are shown). For T-S diagram, see Supplementary Material 3.

below which the temperature remained stable at 7°C–8°C until the bottom in all fjords except Bal, where it was markedly colder and reached a minimum of 3°C. The pycnocline depth typically coincided with the sill depth for most fjords (Fig. 2), and was most pronounced in narrow fjords with shallow sills, and least pronounced in more open fjords with a deeper/more open sill and a shallower basin depth, such as Malangen and Vaagsfjorden. Surface fluorescence (integrated across the upper 10 m) ranged 0.08–1.58 mg m^{-3} and did not follow any spatial trends. Water temperature was significantly ($P < .001$) correlated with latitude ($r = -0.72$) (Fig. 1). However, several fjords were distinct outliers in this trend, with Malangen (Mal) showing much higher mean temperatures than would be predicted by its far north location, and Vefsnfjorden and Ranfjorden (Vef, Ran) having much lower temperatures than other fjords of the same latitude.

Zooplankton biomass

The total zooplankton biomass varied between 3 and 150 mg DW m^{-3} (mean 21 mg DW m^{-3}) (Fig. 3a, Supplementary Material 4). The highest biomass was observed in the inner part of Malangen, where it was two times higher than the next highest value (Balsfjorden). The best model predicting total biomass, as well as biomass of the 1–2 mm and >2 mm size fractions, included only latitude, with higher values observed at the more northern locations (Supplementary Material 5). The biomass of the <1 mm zooplankton

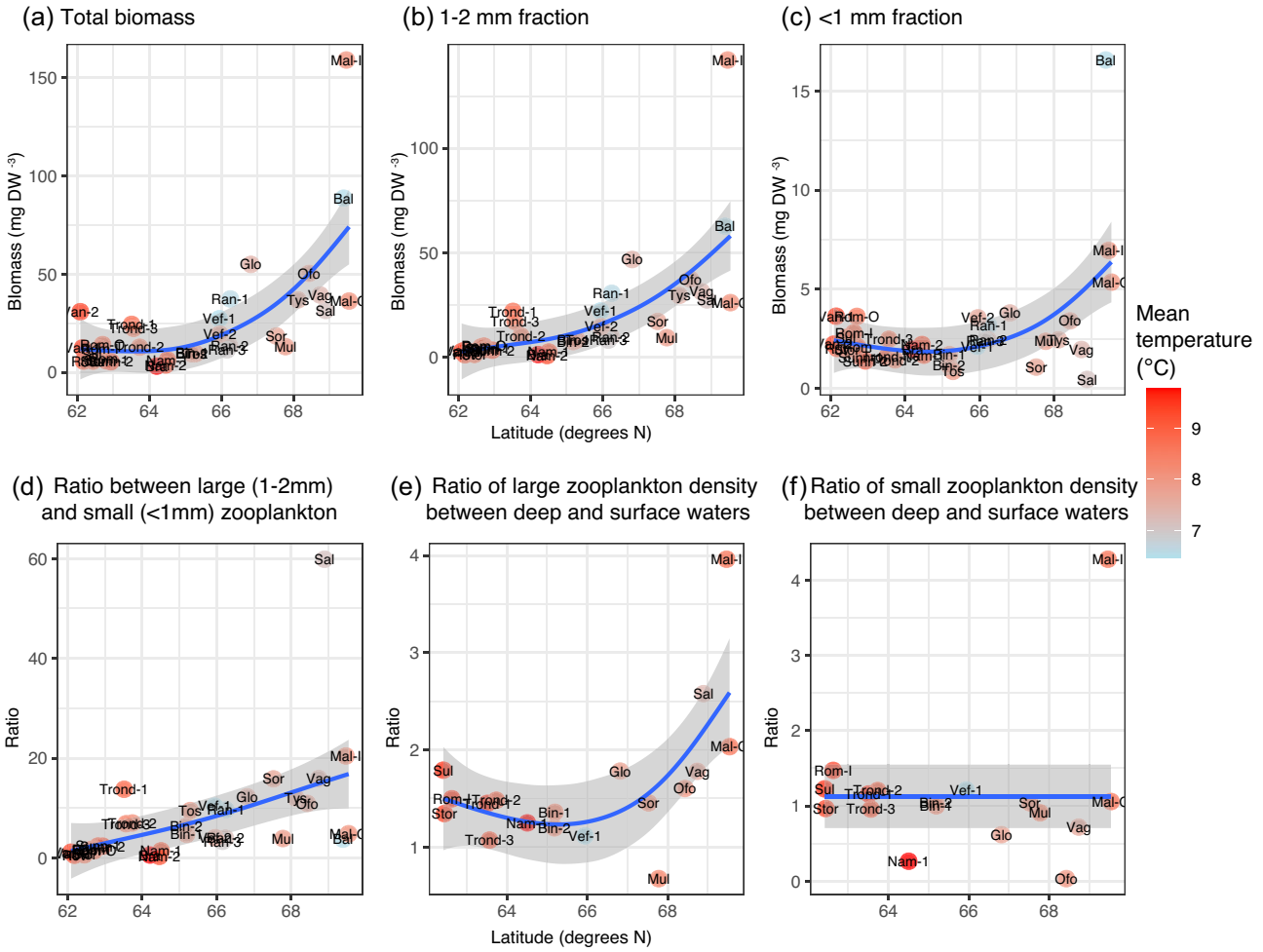

Figure 3. Latitudinal trends of (a) biomass (mg DW m^{-3}) of total zooplankton, (b) biomass density (mg DW m^{-3}) of 1000–2000 μm size fraction, (c) biomass density of <1000 μm size fraction, (d) ratio between large (1000–2000 μm) and small zooplankton biomass, (e) ratio of large (1000–2000 μm) zooplankton biomass density of deep (>200 m) and vs. shallow (<200 m) waters; (f) ratio of small (<1000 μm) zooplankton biomass density (mg DW m^{-3}) of deep (>200 m) vs. shallow (<200 m) waters. Solid lines indicate the GAM fit between the two parameters, grey band indicates the 95% confidence interval for the regression.

fraction was also correlated to latitude (Fig. 3c), but the best model via AIC included surface temperature and fluorescence (Supplementary Material 5). The latitudinal trend was particularly pronounced above 66°N and was driven primarily by the 1–2 mm fraction ($P < .001$; $R^2 = 0.61$) (Fig. 3a, b). The ratio between large (1000–2000 μm) and small (<1000 μm) mesozooplankton was also positively related with latitude ($P < .01$; $R^2 = 0.39$), indicating a relative dominance of larger organisms at higher latitudes (Fig. 3d). The macrozooplankton (>2 mm) showed a non-linear relationship with latitude (Fig. 4), with higher values in the southernmost and northernmost locations. Different organisms contributed to the macroplankton in different parts of the study area—in the north, it was dominated by chaetognaths and crustaceans, while in the southern locations, it was composed primarily of gelatinous plankton (siphonophores, hydrozoan jellyfish, and ctenophores) and sea star larvae (*Luidia sarsii*) (Fig. 4, Supplementary Material 4). Ctenophores and scyphozoan jellyfish were observed in large volumes (>1 ml m^{-3}) in Vagsfjorden (Vag), Salangen (Sal), and Nordfolda (Mul);

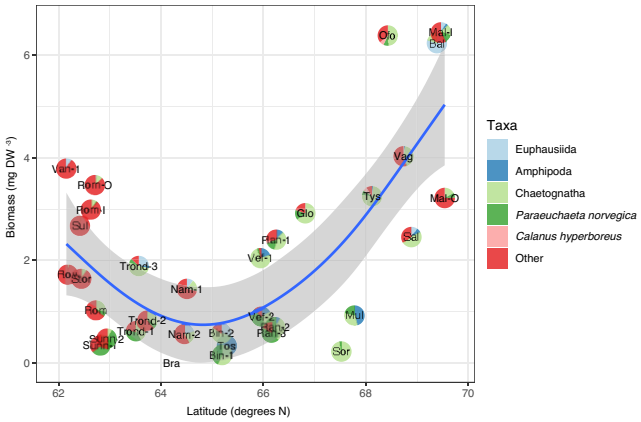

Figure 4. Latitudinal trend of macrozooplankton (>2 mm) biomass. Solid lines indicate the GAM fit between the two parameters, grey band indicates the 95% confidence interval for the regression.

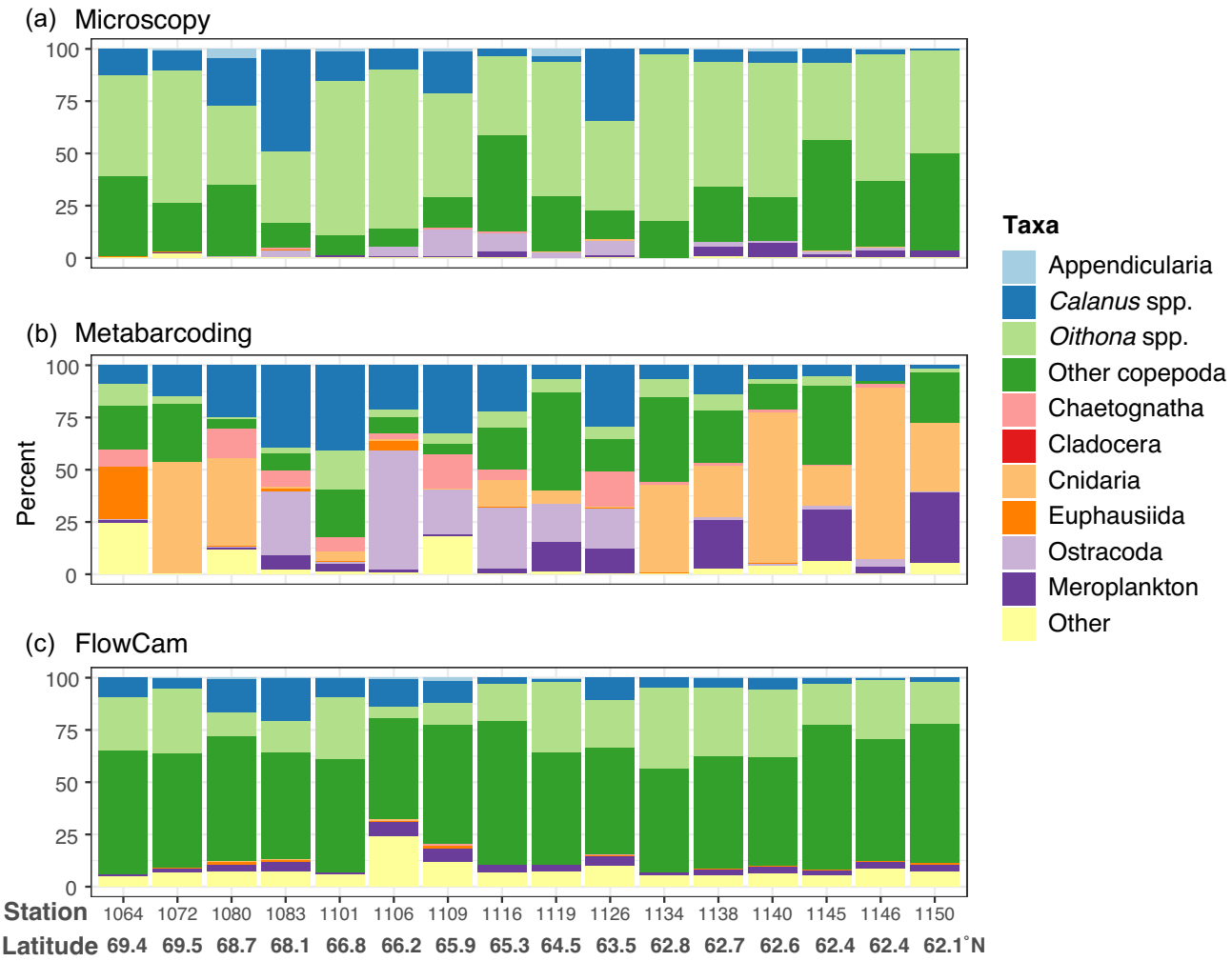

Figure 5. Relative taxonomic composition as determined by (a) microscopy, (b) metabarcoding, and (c) FlowCam image analysis.

their contribution in other fjords did not exceed 0.25 ml m^{-3} (Supplementary Material 6).

Among the stations deeper than 200 m, zooplankton was typically concentrated in the deepest layer, with up to 90% of total biomass concentrated below 200 m (mean 70%, median 76%). This was particularly pronounced in the large (1000–2000 μm) zooplankton, where on average 75% of the biomass was found in the deep layer, while only 50% of the small zooplankton (<1000 μm) was found below 200 m. When accounted for total depth, the density of large zooplankton (mg DW m^{-3}) below 200 m was, on average 7 times higher (max = 28) (Fig. 3e) than in the surface layer. The density of small zooplankton was a lot more evenly distributed between the two depth layers, with only one station (Mal-I) showing a concentration of zooplankton 8 times higher at depth (Fig. 3f).

Microscopy counts

The overall zooplankton abundance ranged between 300 and 1700 ind m^{-3}. It had a strong correlation to total biomass (r = 0.82) and followed the same latitudinal trends, with decreasing total abundance from north to south. A total of 53 holoplanktonic and 10 meroplanktonic species/taxa were registered, with the diversity at individual stations ranging between 21 and 47 species/taxa per station (Supplementary Material 7). Small copepods, especially *Oithona similis*, dominated the abundance at most stations (Fig. 5a). *Calanus* spp. (*C. finmarchicus/glacialis* and *C. helgolandicus*) made up 10% or more of the abundance in the northern fjords and in Trondheimsfjorden, but its contribution to overall zooplankton numbers in the other locations was low. The *Calanus* population consisted predominantly of the C5 stage at all stations except Glomfjorden (Glo), where the contribution of C5 copepodites was <2%, and the population was dominated by C4 and C3 copepodites. Ostracods contributed substantially (5%–15%) in the mid-latitude fjords, and meroplankton made up to 5%–7% of zooplankton in the southernmost sampling locations. The numerical contribution of the remaining groups was low, not exceeding 1%–2% (Fig. 5a). Abundance of *Calanus* spp. was highly correlated to the biomass of the 1000–2000 μm fraction ($P < .001$, $R^2 = 0.75$), but there was no correlation between the microscopy-derived abundance and dry weight of any of the macroplankton categories.

Metabarcoding

The sequencing after all the filtering steps produced 2270 960 reads, which corresponded to between 520 00 and 257 000 reads per sample. Rarefaction curves suggested that this

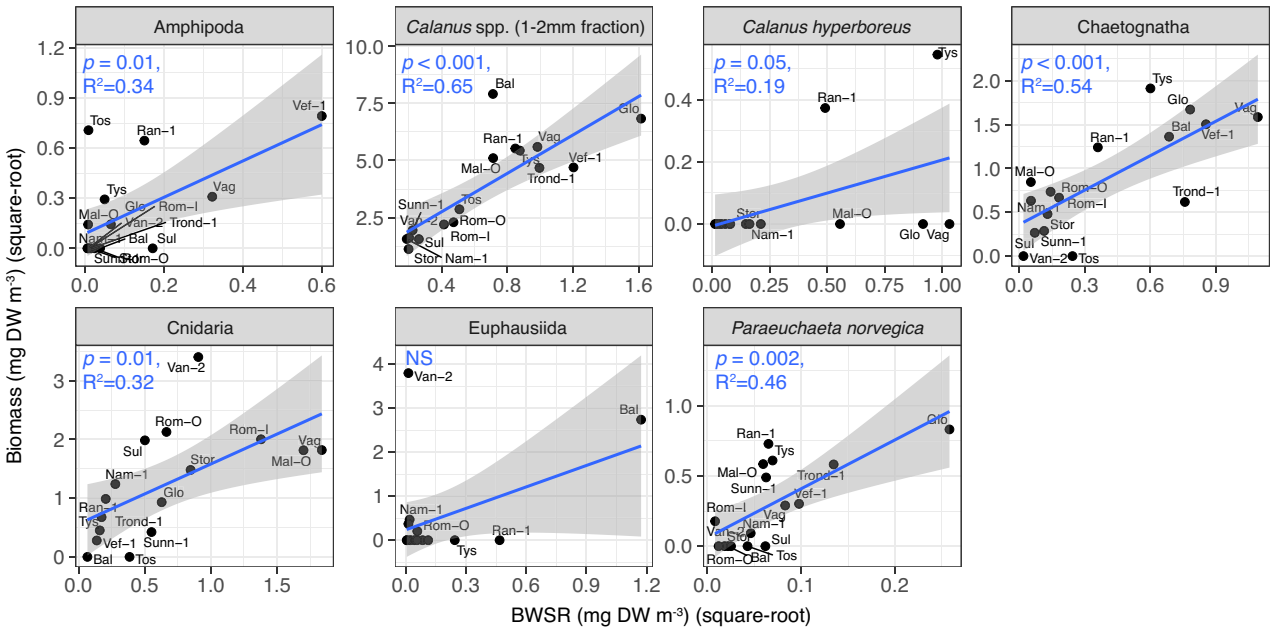

Figure 6. Relationship between square-root transformed dry weight of macrozooplankton and biomass weighed sequence reads (BWSR). *Calanus* spp. corresponds to the 1000–2000 μm biomass fraction. Lines indicate linear regression fit; gray ribbons indicate 95% confidence interval of regression line. Note that different fractions of the sample were used to obtain the two estimates.

sequencing depth was enough to recover almost all diversity in all but two samples (1116 and 1126) (Supplementary Material 8). The sequences clustered into 479 MOTU's, of which 161 were identified as holoplanktonic organisms, 99—as meroplankton (benthos or fish), 68—as phytoplankton, 17—as non-planktonic species, and 134 were unknowns. The holo- and meroplanktonic MOTU's accounted for 87.5% and 8.5% of total reads, respectively, while unknowns made up 2.5% of total reads. The zooplankton MOTU's corresponded to 97 unique holoplanktonic and 92 meroplanktonic species/taxonomic categories. These included 40 copepod species, 22 species of cnidarians, 5 species of euphausiids, and 4 species of amphipods (Supplementary Material 9).

Most of the species identified via microscopy were also present in the rarified metabarcoding data. Exceptions included the appendicularians *Fritillaria borealis* and *Oikopleura* sp., *Microsetella norvegica* (present at two stations), *Gaetanus tenuispinus* (present at one station), and *G. brevispinus* (present at one station). Compared to microscopy-derived abundance data, the relative sequence read abundances of the different taxa were very variable between stations. Copepods, on average, made up only 50% of total reads, and several stations were dominated by other taxa. For example, the mid-latitude stations contained 25%–50% reads of Ostracoda, and the southern stations contained up to 80% DNA of Cnidaria, mostly due to the presence of the siphonophore *Nanomia cara*. It is noteworthy that siphonophore fragments were also observed visually within the formalin-preserved samples but colonies were only counted quantitatively when pneumatophores were encountered, which could partially explain this discrepancy between the two datasets. Meroplankton was also more prominent in the metabarcoding dataset, with a relative contribution of 15%–30% at the more southern locations. These high contributions were mainly driven by the sea star *L. sarsi*.

Overall BWSR trends of individual copepod species largely mirrored the abundances recovered by microscopy (Fig. 6). Additionally, BWSR allowed to differentiate between species where it was not possible to do so morphologically, e.g. to distinguish species of meroplankton and ostracods, or between *C. finmarchicus* and *Calanus glacialis* (Fig. 7) and to identify *Pseudo/Paracalanus* spp. species. BWSR was also significantly correlated to the dry weight of the manually sorted taxa of macroplankton with the exception of Euphausiids (Fig. 8), and the 1000–2000 μm biomass fraction was significantly correlated to the BWSR of *Calanus* spp.

FlowCam

The total abundance and biovolume recovered by the FlowCam were strongly correlated to microscope-derived abundance ($r = 0.91$) and total dry weight ($r = 0.87$), respectively. The normalized biovolume size spectra (NBSS) slopes ranged from −0.87 to −0.35 and showed a significant relationship with latitude ($P < .05$, $R^2 = 0.31$), and an even stronger relationship to mean water temperature ($P < .05$, $R^2 = 0.5$, reflecting the "outliers" in the latitudinal temperature trends: Vef and Ran, which were much colder relative to what was predicted by their geographical position and Mal, which was much warmer (Fig. 9). The NASS slopes ranged from −1.85 to −1.35 and followed identical patterns to NBSS. The lowest slope values were observed at warmer temperatures/lower latitudes, indicating a relative community dominance of smaller organisms at those locations and consistent with the trend shown by the ratio between large and small dry weight fractions. The NBSS and NASS intercepts, which can serve a proxy for total zooplankton biovolume/abundance, respectively, similarly showed a clear trend of increasing values with latitude/lower water temperature ($P < .01$, $R^2 = 0.61$) (Fig. 9), mirroring both the microscopy-derived abundance and dry weight biomass data. The biovolume of

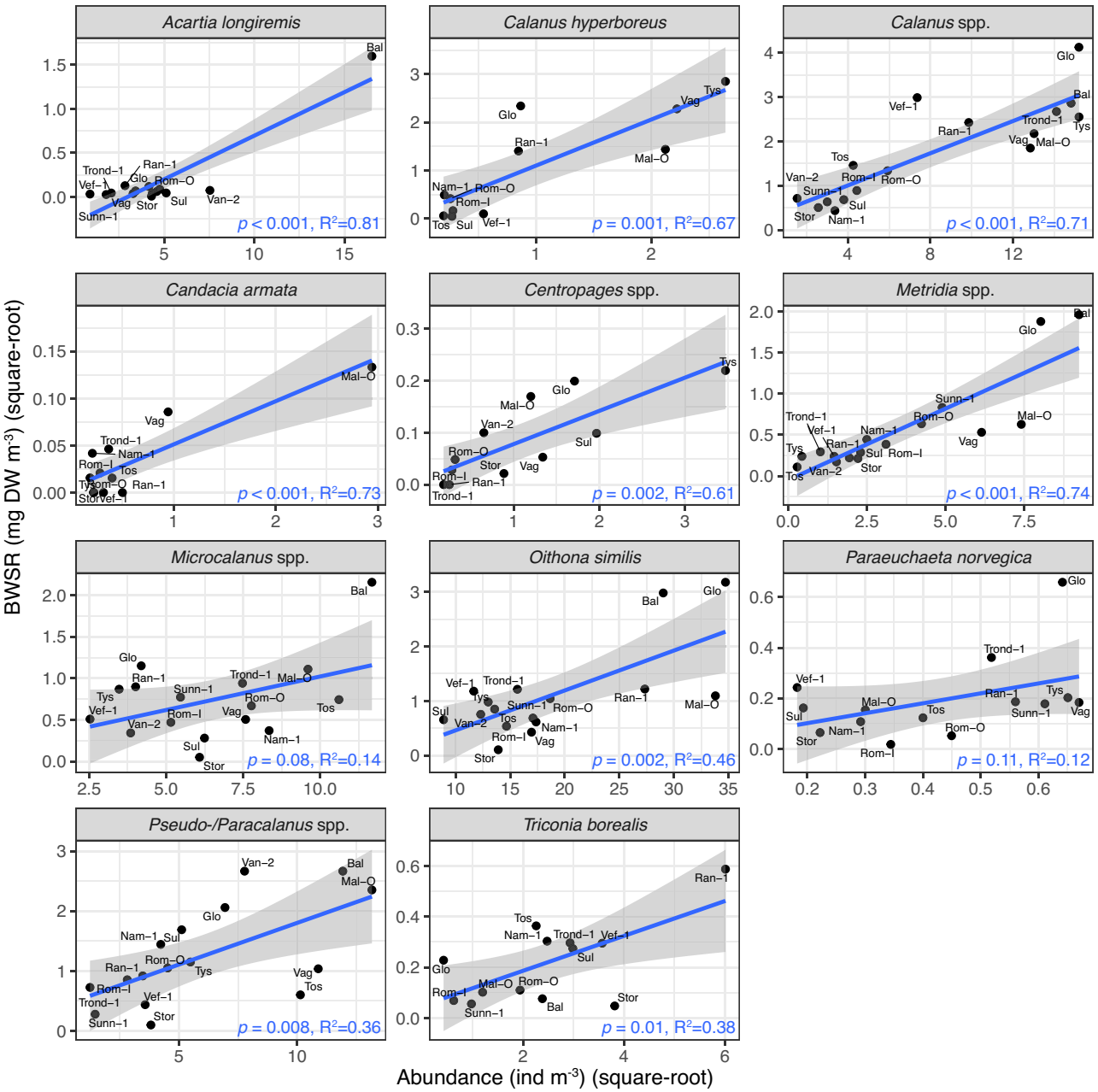

Figure 7. Relationship between square-root transformed species abundance (miscroscopy-derived) and square-root transformed BWSR (metabarcoding/dry weight derived). Lines indicate linear regression fit; gray ribbons indicate 95% confidence interval of regression line.

200–1000 μm and 1000–2000 μm fractions was also highly correlated with the respective size fractionated dry weights ($P < .001$, $R^2 = 0.65$ and 0.92, respectively), supporting the notion that biovolume can be used as proxy for biomass.

Taxonomic classification of organisms identified 12 unique groups, of which three copepod categories (*Calanus* spp., *Oithona* spp., and Calanoida) heavily dominated the abundance at all stations (Fig. 5c). Although the FlowCam image analysis showed an overall lower contribution of *Oithona* and *Calanus* compared to microscopic analysis of the same samples (Fig. 5c), the trends in the relative contribution of major taxonomic groups among samples were consistent between the methods. Meroplankton contributed 3%–5% at most stations, and other holozooplanktonic organisms made up 5%–25% of total abundance.

Community analysis

The nMDS of species abundance data (microscopy-derived) and the species BWSR (metabarcoding/dry weight derived) revealed very similar patterns (Fig. 10). Latitude and mean water temperature were correlated with the first axis, while bottom depth drove the separation along the second axis. Both datasets separated the fjords into three broad groups—a Northern Group (Bal, Mal, Glo, and Vaag), a Southern Group (Stor, Van, Sul, Rom, Ting, and Nam), and a Deep-Water Group (Vef, Ran, Tys, and Tos). Only Trond was grouped with the Deep-Water Group within the BWSR dataset and the Southern Group in the microscopy-derived abundance dataset. Additionally, Malangen (Mal) was much closer to the Southern Group in the BWSR data. The species responsible for separating the groups partially, but not

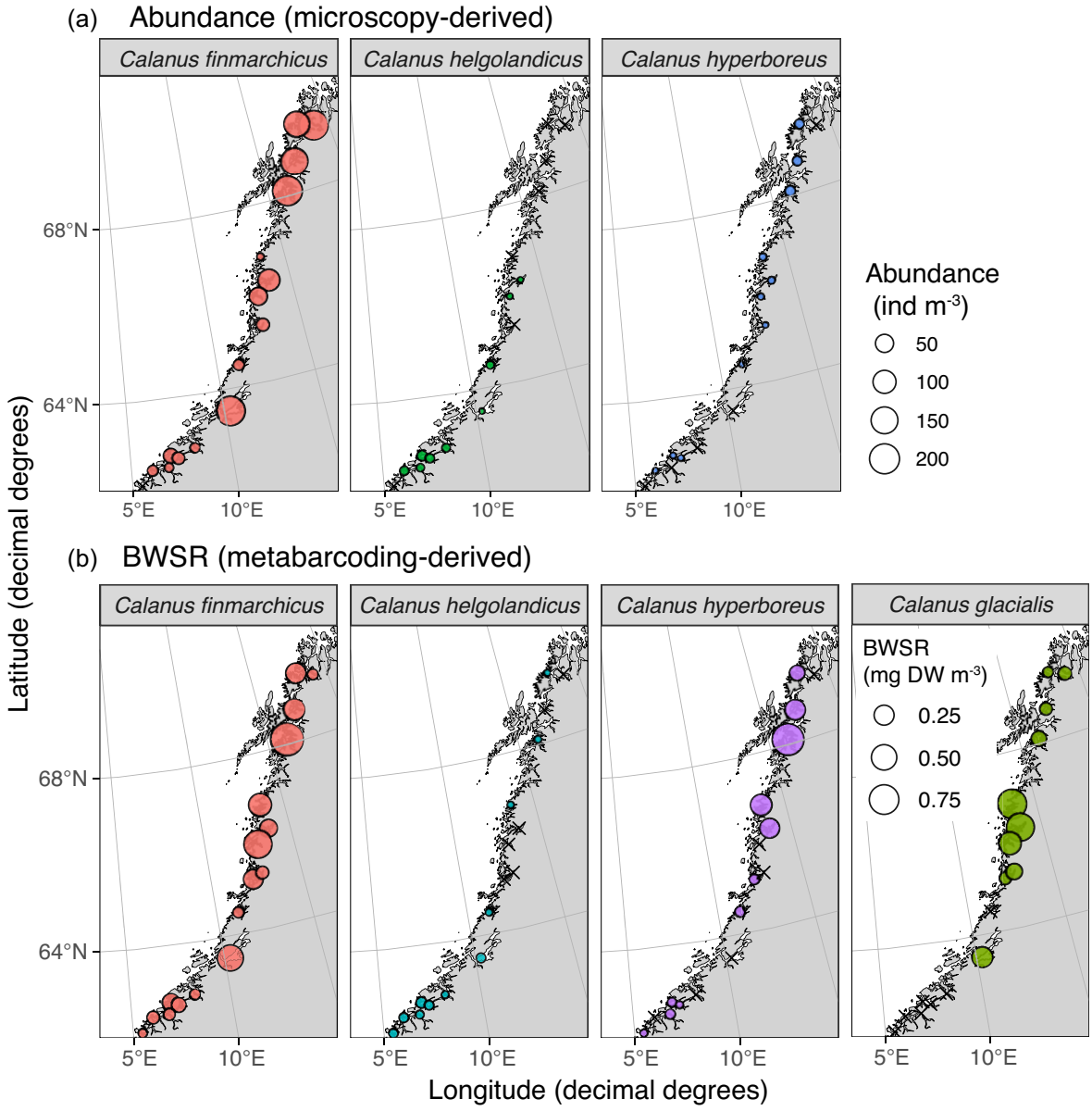

Figure 8. Spatial distribution of *Calanus* species; (a) abundance of C5/adult females derived from microscopy, (b) BWSR derived by metabarcoding (all stages).

completely, overlapped between the two datasets. Both datasets identified *Metridia* spp., *Thysanoessa inermis*, *Sagitta elegans*, *Calanus hyperboreus*, *C. finmarchicus*, *Pseudo/Paracalanus* spp. (identified as *Pseudocalanus acuspes*, *P. minutus*, *P. moultoni*, and *P. parvus* in the metabarcoding data) as the species driving the Northern Group. The metabarcoding data additionally identified the pelagic polychaete *Tomopteris* sp., the chaetognath *Eukrohnia hamata*, and the copepod *C. glacialis*, while the microscopy data identified the appendicularian *Oikopleura* sp., *M. norvegica*, and *Temora longicornis* as significantly driving the communities. The Southern Group was distinguished by the presence of *Calanus helgolandicus* and meroplankton; metabarcoding additionally identified *Ctenocalanus vanus* and *Pseudocalanus elongatus*. The Deep-Water Group was characterized by the presence of ostracods in both datasets (*Boroecia borealis* and *Discoconchoecia elegans* in the metabarcoding data). The microscopy also identified the copepods *Paraeuchaeta norvegica* and *Heterorhabdus norvegicus* and the amphipod *Themisto abyssorum* in the Deep-Water Group; metabarcoding identified the jellyfish *Periphylla periphylla* and the copepods *Triconia borealis*, *Candacia norvegica*, and *Spinocalanus longicornis*.

Biogeographic affinity

Based on relative sequence counts, there was a clear latitudinal trend in the biogeographic affinity (Supplementary Material 10) of the taxa composing the communities (Fig. 11). Arctic/Arcto-boreal species typically dominated the communities in the northern fjords, where they composed 50%–75% of all sequence reads. Their relative contribution declined with latitude, and they made up 5%–10% of sequence reads at the four southern-most stations. Boreal species showed variable representation (10%–60%) with no clear spatial trends. The contribution of cosmopolitan species ranged between 5% and

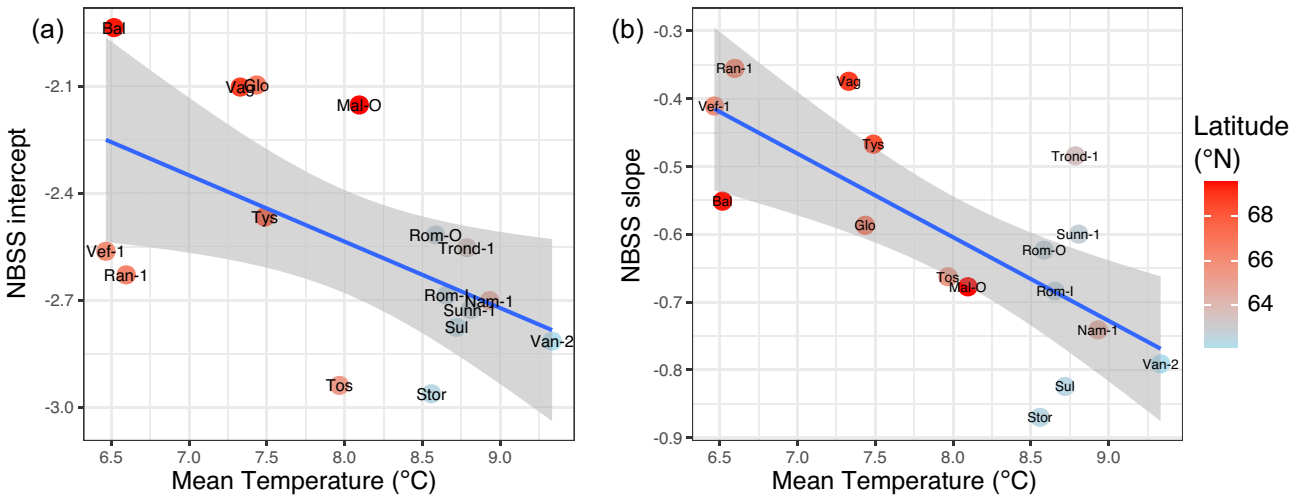

Figure 9. Water temperature vs. normalized biomass size spectrum (NBSS) (a) intercept and (b) slope. Lines indicate linear regression fit; gray ribbons indicate 95% confidence interval of regression line. Color indicates mean latitude.

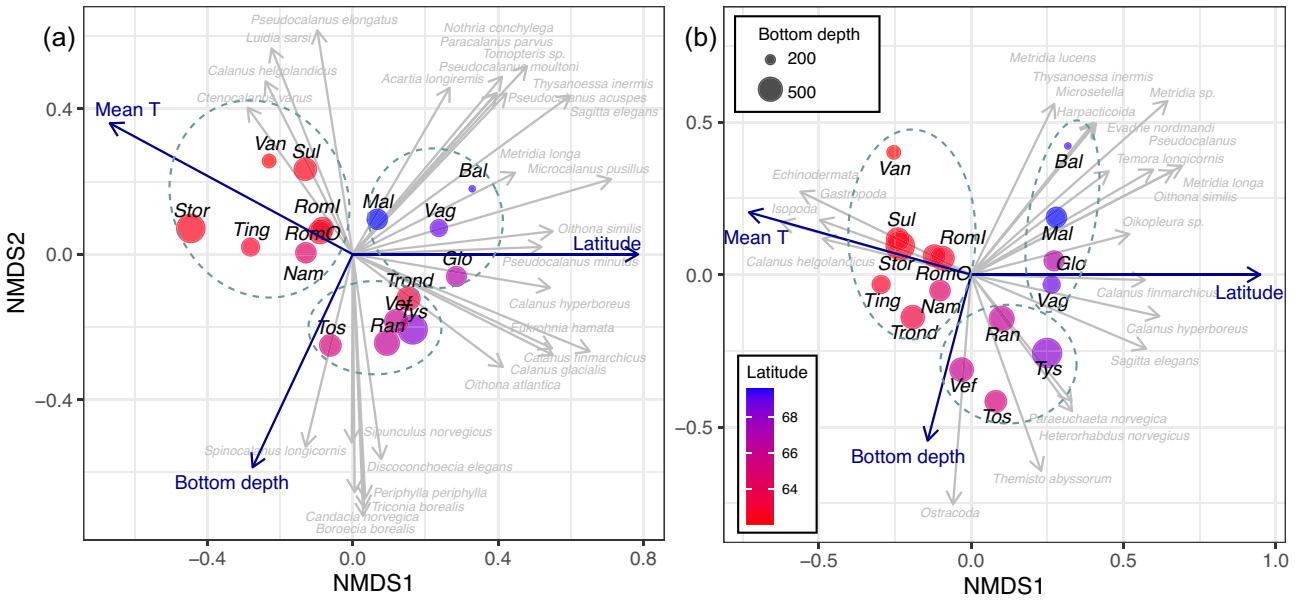

Figure 10. nMDS of (a) square-root transformed abundance (microscopy-derived) and (b) BWSR (metabarcoding/dry weight derived) data. Arrows and text indicate biplots with arrow length proportional to the strength of the relationship; gray arrows and text show species driving the ordination, while blue shows physical parameters significantly correlated to the ordination. Symbol size represents bottom depth, and symbol color represents latitude.

25% in northern fjords and increased markedly to comprise up to 80% of communities in some of the southern fjords. Malangen was a clear outlier, with only 25% of reads belonging to Arctic/Arcto-boreal species, despite its location in the far north, and with nearly 50% composition of sequence reads belonging to cosmopolitan species. Temperate/warm-water species were mostly observed in the more southern locations, with a low overall contribution (never exceeding 15%). Taxa with an unknown distribution (typically those that could not be identified to species level) made up 1%–25% of sequence reads.

Discussion

We captured the zooplankton communities across our study area entering their winter state, as marked by the reduced chlorophyll levels, a notable accumulation of zooplankton biomass below 200 m, and the predominance of the diapausing C5 stage of *C. finmarchicus*. Our results, therefore, should be interpreted within this seasonal context.

Zooplankton community structure, environmental influences, and implications for overwintering

Our findings highlight distinct latitudinal trends in zooplankton communities both in total amounts of zooplankton observed and relative taxonomic composition. Although latitude itself does not directly influence biological systems, it can serve as a useful proxy for other parameters. In our case, latitude was highly correlated to water temperature, as well as reflected relative timing of the productive season, here defined as the part of the year with hightened primary and secondary

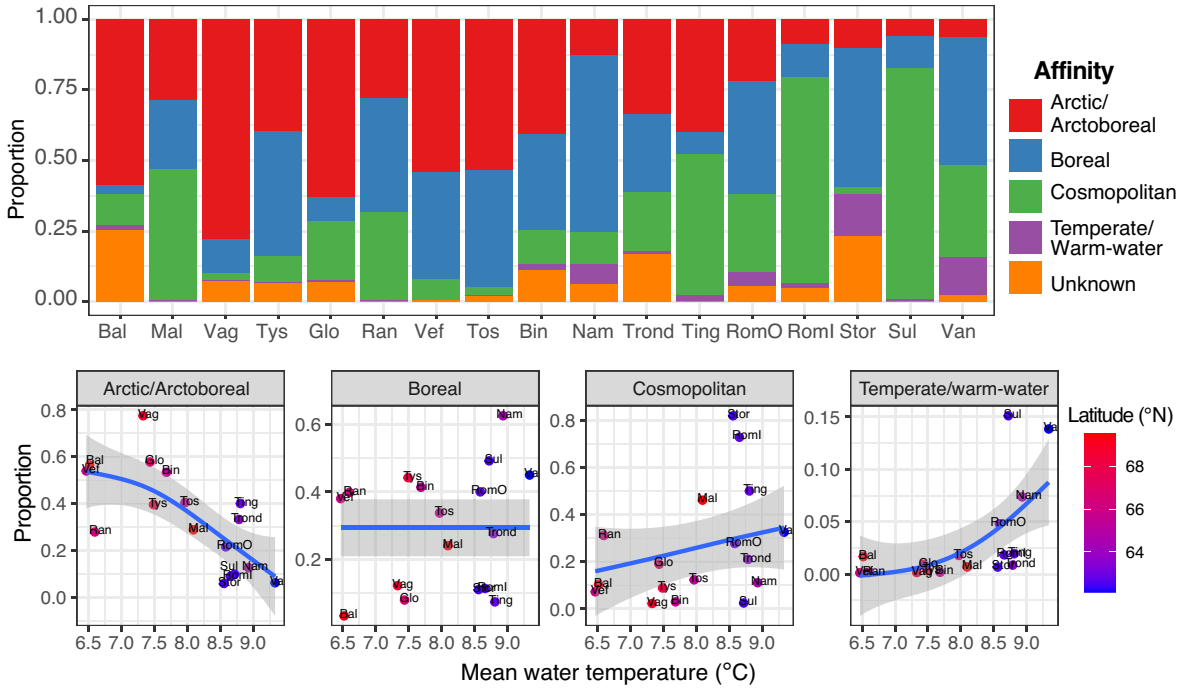

Figure 11. Relative sequence read counts belonging to different biogeographical groups and relationship of proportion of each group to mean water temperature.

production. We observed higher zooplankton abundance and biomass at more northern locations relative to locations in the south; higher latitudes were also correlated with higher NBSS slopes and a larger relative contribution of larger mesozooplankton biomass, reflecting a relatively higher importance of larger organisms toward the north. In terms of community composition, from south to north, the community shifted from one dominated by small copepods, meroplankton, and gelatinous plankton to one with a higher contribution of *Calanus*, chaetognaths, and crustacean macroplankton. The relative contribution of Arctic and Arcto-boreal species increased with latitude, while cosmopolitan and boreal species declined. These patterns may reflect both true geographical trends, as well as the relative timing of the seasonal transitions at different locations. For example, the relatively high contribution of meroplankton and siphonophores at lower latitudes may reflect the longer productive season at those locations. The higher dry weight and biovolumes observed at higher latitudes align with global trends that show zooplankton biomass to increase in polar/sub-polar waters (Moriarty et al. 2013, Drago et al. 2022). However, we cannot exclude that these patterns within our study area may be specific to the studied season or year.

The trends in biomass were highly influenced by the relatively large copepod *C. finmarchicus*, which is distributed throughout the North Atlantic, but has an overwintering center in the deep Norwegian Sea (Melle et al. 2014), adjacent to our study region. It can also overwinter in fjords along the northern part of the Norwegian coast (Espinasse et al. 2016, Coguiec et al. 2023), and the high biomass observed at northern locations likely represents these overwintering populations. The local oceanography may play a key role in facilitating the advection and subsequent retention of overwintering zooplankton within fjords (Backhaus et al. 1994, Falkenhaug et al. 1995, Samuelsen et al. 2009, Gao et al. 2024). More specifically, the Norwegian Coastal Current undergoes a coastward shift in its shear during the autumn months (Sætre 2007), enhancing the influence of this water mass in coastal regions. Consequently, zooplankton from the Norwegian Sea may be transported into the fjords, where they can sink below sill depth and avoid being flushed back out onto the shelf (Gao et al. 2024). The biomass of the 1–2 mm fraction, primarily consisting of *C. finmarchicus*, was notably high in many of our sampled locations, particularly in the north, often nearing or exceeding those reported for regions recognized as key distribution areas of this species. According to Melle et al. (2014), "population centres" of *C. finmarchicus* are defined as locations where overwintering populations exceeded 15 000 ind m^{-2}, which, based on our data, roughly corresponded to 4.2 g DW m^{-2}. In our study, 15 out of 34 fjord locations sampled exhibited biomass values of the 1–2 mm fraction that surpassed this threshold, with over half of those exceeding 10 g DW m^{-2} and one location (Malangen) having a biomass of 32 g DW m^{-2}. Among the stations where microscopic counts were taken, 9 of 16 locations had *Calanus* abundances exceeding 15 000 ind m^{-2}, with the maximum observed in Tysfjorden (161 000 ind m^{-2}). These findings are noteworthy because the fjord depths are much shallower than the typical key overwintering habitat of *C. finmarchicus*, which is usually deeper than 600–800 m (Melle et al. 2014). The exceptionally high biomass of *C. finmarchicus* in Malangen, e.g. occurred at a depth of only 380 m. This is consistent with earlier studies, which found up to 180 000 ind m^{-2} overwintering *Calanus* in Malangen in October 1992 (Falkenhaug et al. 1997). These overwintering fjord populations may be important reservoirs that seed surrounding shelf waters with zooplankton in the spring. The overwintering *Calanus* in fjords produce eggs and nauplii that rise to the surface and are carried out to the shelf, where they can resupply local populations and be an important food source for larval cod (Espinasse et al. 2016).

Table 2. Summary of strengths and limitations of the four methodologies employed in this work.

Method	Strengths	Limitations	Best applications
Dry weight	• Easy and quick to measure • Quantitative proxy of zooplankton total amount/ratio between size classes	• No/very low taxonomic resolution • No abundance information • Prone to bias (i.e. phytoplankton blooms and other debris)	• Total/size-fractionated zooplankton biomass estimates across large spatial/temporal scales
FlowCAM image analysis	• Less time consuming than microscopy • Size and biovolume distribution information • Total abundance information	• Low taxonomic resolution • Low accuracy of taxonomic assignment even at low taxonomic resolution • No developmental stage information	• Total zooplankton abundance estimates across large spatial/temporal scales • Size/trophic structure of the communities
Microscopy	• High taxonomic resolution • Species-specific and total abundance information • Developmental stage composition	• Some groups underrepresented (i.e. gelatinous species) • Very time consuming • Prone to human bias	• Total community structure • Species population structure, life history and phenology • Biodiversity estimates (focused on certain groups)
Metabarcoding	• Highest taxonomic resolution • Quantitative proxy for species biomass • Shows similar community patterns to microscopy data • Less time consuming than microscopy	• No abundance information • No developmental stage information • Risk of false positives • Some groups underrepresented, multiple barcodes may be needed • Requires dedicated facilities • Relatively high reagent costs	• Total community structure • Biodiversity estimates (all groups) • Detection of rare or cryptic species and groups

The latitudinal pattern in size structure within the communities was also consistent with global trends that show a strong negative correlation between habitat temperature and individual body mass, both within entire communities and individual species (Evans et al. 2020, Brandão et al. 2021). The temperature/latitude-associated gradient in size classes that we observed was likely a combination of both a taxonomic shift in the communities to larger species (i.e. from small copepods to *Calanus* spp.) as well as a shift to larger sizes within the *Calanus* copepods themselves (Horne et al. 2016). In general, metabolic rates are lower in colder waters, so zooplankton may be able to allocate more energy to growth and reproduction rather than maintenance (Clarke and Fraser 2004). Additionally, a larger body size, often associated with increased energy storage capabilities, may be advantageous in environments with extreme seasonal productivity fluctuations (Evans et al. 2020). This variation in size structure can have substantial implications for trophic interactions and energy transfer efficiency within the ecosystem, since many predators choose their prey based on size. For example, Beaugrand et al. (2003) found the decline in cod recruitment in the North Sea related to a shift to smaller zooplankton. García-Comas et al. (2016) also underscore the importance of size structure in planktonic communities, showing that higher predator size diversity enhances trophic transfer efficiency, particularly in planktonic communities where prey size diversity is high.

The structure of the fjord, the depth of the sill, as well as the seasonal variations in the coastal currents, determine the extent that it is influenced by external water masses from outside of the fjord. In our study, an example of this was Malangen, which, despite being the northern-most sampled location, was markedly boreal in character, both in terms of water properties and species composition. The open structure of this fjord facilitates water exchange with surrounding shelf waters, sharply contrasting with the neighboring Balsfjorden (Falkenhaug et al. 1995). Deeper fjords can also provide refugia for deep-water and Arctic-relic species, as evidenced by the deep fjord locations in our study clustering separately based on community composition, despite the integrated nature of our net tows. However, while the structure of fjords, such as depth, width of the fjord opening, or sill depth, undeniably shape their biological communities on smaller geographical scales (i.e. Aksnes et al. 1989, Gorsky et al. 2000, Hosia and Båmstedt 2008), the broad-scale geographical patterns we observed significantly overshadowed these structural influences. Despite expectations to the contrary, outside of the above-mentioned examples, we found little correlation of biological patterns to structural characteristics of the examined fjords. This finding cautions against the oversimplification of extrapolating parameters from a single fjord system to other fjords along the Norwegian coast in ecological monitoring efforts, advocating for a nuanced understanding of each system's unique characteristics.

Comparative efficacy of applied methodologies

The integration of several different methods allowed us to examine a large range of zooplankton parameters from samples collected by a single net tow. Our data included total and size-fractionated biomass, species and total abundance, size structure, taxonomic diversity at a very high level of resolution as permitted by DNA analysis, and developmental stage composition. Each of the methodologies we used in this work provides distinct advantages but also has clear limitations when applied individually, as summarized in Table 2.

Size-fractionated bulk dry weight measurements, for instance, offer an highly inexpensive and time-effective method to examine overall trends and patterns in zooplankton biomass distribution, despite not providing species-level data. As this has been one of the most widely implemented method to measure zooplankton since the 1960s (Harris et al. 2000), it also provides a useful metric to compare with historical data. Although this approach provided taxa-specific estimates only for the macroplankton, it has been established that the

1000–2000 µm size fraction in Norwegian waters consists primarily of *C. finmarchicus* stage CV and adults (Skjøldal 2021), which is further supported by the strong correlation between this biomass fraction and *Calanus* abundance and BWSR within our data. Since *Calanus* is the main contributor to overall zooplankton biomass in most marine environments in Norwegian waters (Wiborg 1955), this provides a very useful and easily obtained proxy of this key species.

Conversely, microscopy offers precise species-specific abundance data and detailed stage composition for certain species; however, this technique remains labor-intensive and prone to human error and bias. Although there have been few published efforts to quanitify the error rates associated with manual microscopic sorting, one study highlights the challenges faced by human taxonomists in identifying marine dinoflagellates, revealing that even trained personnel achieve only 67%–83% self-consistency and 43% consensus between experts (Culverhouse et al. 2003). Microscopy is also less effective for identifying groups that do not preserve well or lack sufficient distinguishing features for accurate identification. Even within well-studied groups such as calanoid copepods, species-level identification is typically only feasible at the adult stage, although adults often compose a small percentage of the population (Ershova et al. 2017), and groups like meroplankton are at best identified to class or phylum.

COI metabarcoding can produce a very high level of taxonomic resolution and can identify individuals at any stage of development, although depending on the barcoding region/primer set used, it may also exclude or underrepresent certain groups, some of which may be ecologically important. The quantitative interpretation of metabarcoding data has historically been, and remains, a controversial subject (Bucklin et al. 2016), but in this study we apply a tested protocol that proved to be effective at relative quantification of most groups of marine zooplankton (Ershova et al. 2023). Although metabarcoding remains unsuitable for estimating species abundances directly, relative sequence counts are fairly well correlated to relative species biomass for most taxonomic groups. When combined with a bulk biomass measurement, this approach can generate a semi-quantitative metric that is akin to species biomass (BWSR) (Ershova et al. 2023). The systematic discrepancy between relative sequence read counts and relative abundance was clear, e.g. in the much higher relative proportions of *C. hyperboreus* within the metabarcoding data relative to the microscopy data (Fig. 8). The high relative sequence counts of *L. sarsii*, a large-bodied sea star larva, also reflect how a few large individuals can disproportionately contribute DNA relative to their actual abundance. While the metabarcoding recovered a lot of cryptic diversity, it also failed to identify some taxonomic groups completely, such as appendicularians and certain species of copepods and siphonophores. For example, the siphonophore species *Dimophyes arctica* or *Lensia conoidea*, which were identified within the macroplankton biomass fraction and are known to be numerous in the fjords during the fall, were absent in the sequencing data. This suggests that our chosen primers may not be ideal for capturing all members of these groups, and other primers and/or barcodes should be included if these taxa constitute groups of interest. Remaining gaps in reference libraries may also account for some of the missing taxa, although the zooplankton of the North Atlantic is one of the best barcoded groups in the world (O'Brien et al. 2024).

Finally, FlowCam image analysis is highly time-effective and provides rapid information of total abundance, size-spectra, and individual biovolume, but its current ability to identify taxa beyond a very broad grouping remains limited. This is expected to improve in the future as training datasets and deep-learning algorithms continue to develop and become more and more sophisticated. However, the level of taxonomic information gained from a two-dimensional image, randomly imaged in a fluid flow, can never approach the same level of taxonomic depth as proper microscopic analysis. Nevertheless, even without taxonomic assignment, mesozooplankton abundance and biovolume size spectra can provide important insights on community productivity and other ecological processes. For example, plankton size spectra have been used to predict biomass and production of higher trophic levels, such as fish communities (Sprules and Barth 2016). As such, this approach has a major advantage in terms of cost and time investments when compared to the other methods described above. The ongoing development of plankton imaging systems will continue to elevate the understanding of how size structure influences the pelagic ecosystems (Dugenne et al. 2023).

Although the integrated approach we implemented circumvents a lot of the limitations that are associated with each individual method, it remains constrained by the sampling design. More specifically, our reliance on a single net tow at one location per fjord inherently limits the scope of our data. Plankton communities can exhibit significant heterogeneity even over small spatial scales (Steele 1978), which means that a single sample likely does not fully capture the diversity and abundance variations present within a location. While nets remain a standard tool for plankton sampling, they have issues such as avoidance by larger or more mobile species, destruction of fragile organisms, and variability in catch efficiency depending on the mesh size and towing procedure (Wiebe and Benfield 2003, Skjøldal et al. 2013). Furthermore, net tows typically provide a "snapshot" of the community, which might not accurately reflect larger-scale trends or subtle ecological interactions. Incorporating alternative or complementary sampling methods, such as acoustic surveys or optical plankton systems, could provide additional layers of data to overcome some of these limitations. Acoustic surveys, e.g. can cover larger areas and provide data on the distribution and abundance of some zooplankton groups without physically capturing them, thus offering insights into the spatial dynamics of these populations (Sutor et al. 2005). Optical methods, on the other hand, can offer real-time, *in situ* observations, allowing for the study of plankton without the biases introduced by net sampling (Giering et al. 2022). These can be particularly useful for fragile gelatinous organisms.

Implications of zooplankton monitoring for ecosystem management and conservation

As coastal marine environments, fjords are acutely vulnerable to human impact and climate-related changes, and patterns in species distributions can have critical implications for local biodiversity conservation and ecosystem management. Potential changes in zooplankton composition may have cascading effects on food web dynamics, nutrient cycling, and overall ecosystem functioning (Hays et al. 2005, Steinberg and Landry 2017). Therefore, there is an urgent need for continuous monitoring efforts utilizing integrated methodological approaches to accurately capture these dynamics.

The size structure and relative species composition of the communities can serve as a useful gauge of the extent of the natural spatial and temporal variability, but can also serve as a benchmark against future climate related change. Our results of lower intercepts and steeper slopes of the mesozooplankton size spectra with decreasing latitude (increased temperature) predict increased number of trophic levels, lower assimilation efficiency, productivity, and biomass of higher trophic levels with increasing temperature (Zhou 2006, Sprules and Barth 2016). In our work, warm-water and temperate taxa contributed no more than 15% in the southernmost locations. The strong correlation between water temperature and the relative biogeographic affinity within the communities suggests that the contribution of these taxa may increase and shift northward during warmer years. The dominance of Arctic/Arcto-boreal species in northern fjords, on the other hand, may decline in warmer years as they are replaced by their boreal counterparts. The development of an "index," correlating to the proportion of warm- or cold-water taxa, could serve as a practical and easily implementable tool for comparing ecosystem states over different years or across longer time scales (Beaugrand 2005). However, such assessments hinge on the availability of regularly collected, quantitative, species-level data.

The ability of metabarcoding to distinguish between cryptic species is particularly valuable for tracking range expansions of species and shifts in total biogeographic affinity of communities. Plankton, being passive drifters with currents, can effectively mirror changes in water mass properties or circulation patterns. Yet traditional taxonomy often struggles in this aspect, especially when differentiating species within the same genus, which can be indistinguishable at juvenile stages or and often even at the adult stage. For example, the ratio between the temperate *C. helgolandicus* and the more boreal *C. finmarchicus*, or, farther north, between *C. finmarchicus* and *C. glacialis* has long been used to track the effects of climate change in NwCW (Falkenhaug et al. 2022) and borealization of the Arctic (Polyakov et al. 2020). In fjords, even adults of *C. glacialis* and *C. finmarchicus* are virtually indistinguishable morphologically (Choquet et al. 2018), yet *C. glacialis* represents "local" populations as they are not found on the shelf outside the fjords (Choquet et al. 2017), while the *C. finmarchicus* population likely consists of a mix of local and advected individuals (Bucklin et al. 2000). Despite their morphological similarity, closely related species can occupy different ecological niches, exhibit distinct life cycles and production patterns (Ershova et al. 2021) and can have varying ecological significance for predators. For instance, little auks in Svalbard exhibited a marked preference for *C. glacialis* even when they completely overlapped in distribution with *C. finmarchicus* (Balazy et al. 2023).

Metabarcoding also offered improved detection of gelatinous plankton, which can play a very important role in coastal ecosystems (Hosia 2007) but remain challenging to monitor using traditional methods. The sequencing identified 22 cnidarian and 3 ctenophore species and showed an increased contribution of gelatinous plankton in the southern locations, consistent with the macroplankton biomass findings. Jellyfish blooms of species such as ctenophores (Falkenhaug 1996), the deep-water jellyfish *P. periphylla* (Fosså 1992, Sørnes et al. 2007), and siphonophores (Båmstedt et al. 1998, Hosia and Båmstedt 2008, Knutsen et al. 2018) have been registered in a number of coastal areas in Norway, and can have a profound impact on local fisheries and aquaculture (Bosch-Belmar et al. 2020). For example, the proliferation of *P. periphylla* in Trondheimsfjorden was coincident with reduced catches of cod (Jøssang 2015). Increasing blooms of the toxic siphonophore *Apolemia uvaria* have been causing severe lesions and mass death of salmon in fish farms (Agnalt et al. 2024). Siphonophores in particular are difficult to quantify using traditional methods that rely on abundance data, due to the fact that they are colonial organisms and the consequent uncertainty of what constitutes an "individual." In this respect, metabarcoding may offer a better metric to measure their contribution to planktonic communities as it is a proxy for relative biomass, not abundance. This was evident in the high contribution of sequence reads by the siphonophore *N. cara*, consistent with visual observations during similar times of year, where this species had been found to contribute up to 1000 ind m^{-2} (Gorsky et al. 2000). Yet, as discussed in the previous section, not all siphonophore species were captured via the chosen genetic marker, so other barcodes and primer sets may need to be developed to target these species specifically.

In conclusion, the integration of advanced monitoring techniques, such as metabarcoding and imaging systems, with traditional ecological methods offers a comprehensive approach to understanding and managing coastal planktonic communities. As these environments face increasing pressures from climate change and human activity, monitoring efforts should continue to refine and implement these tools. Additionally, net sampling should be supplemented with techniques that allow to capture more of the patchiness inherent to planktonic systems. This will result in more accurate assessments of plankton and their predators, allowing us to inform sustainable management strategies of these fragile ecosystems.

Acknowledgements

We acknowledge the captain and crew of R/V K.B., as well as E.G. for help with the sampling. We also sincerely thank H.S., I.M., and K.M.-S. for providing help and lab support with the genetic component of the study. We thank the two anonymous reviewers for their meaningful feedback. The collection of data were made possible through the Coastal Survey (Økokotokt kysten) project (number 15639), which is financed by the Department of Fisheries and the Fisheries Research Fund.

Author contribution

T.F. and E.E. conceived the study. T.F. collected the samples. M.M. and G.A. did the microscopic analysis of the formalin-preserved samples. T.B. and M.R. did the FlowCam analysis and analyzed the resulting data. E.E. did the genetic lab work, bioinformatics and overall data analysis. E.E. wrote the manuscript with contributions from all co-authors. All co-authors have read and approved the final version of the manuscript.

Supplementary data

Supplementary data is available at *ICES Journal of Marine Science* online.

Conflict of interest: None declared.

Funding

This work was done with funding from the Norwegian Research Council (Norges forskningsråd) through the CoastRisk initiative (NFR 299554/F40).

Data availability

The data on biomass, microscopy counts, MOTU sequence counts, and FlowCam counts are available in the online supplementary material. The raw sequencing data can be found at NCBI under BioProject PRJNA947953.

References

Agnalt A-L, Diserud OH, Dunlop KM *et al. Risikorapport norsk fiskeoppdrett 2024-Produksjonsdødelighet hos oppdrettsfisk og miljøeffekter av norsk fiskeoppdrett*. Bergen: Havforskningsinstituttet, 2024.

Ahyong S, Boyko CB, Bailly N *et al.* World Register of Marine Species (WoRMS). 2024. https://www.marinespecies.org (1 April 2024, date last accessed).

Akaike H. A new look at the statistical model identification. *IEEE Trans Autom Control* 1974;**19**:716–23. https://doi.org/10.1109/TAC.1974.1100705

Aksnes DL, Aure J, Kaartvedt S *et al.* Significance of advection for the carrying capacities of fjord populations. *Mar Ecol Prog Ser* 1989;**50**:263–74. https://doi.org/10.3354/meps050263

Álvarez E, López-Urrutia Á, Nogueira E. Improvement of plankton biovolume estimates derived from image-based automatic sampling devices: application to FlowCAM. *J Plankton Res* 2012;**34**:454–69. https://doi.org/10.1093/plankt/fbs017

Álvarez E, Moyano M, López-Urrutia Á *et al.* Routine determination of plankton community composition and size structure: a comparison between FlowCAM and light microscopy. *J Plankton Res* 2014;**36**:170–84. https://doi.org/10.1093/plankt/fbt069

Backhaus JO, Harms IH, Krause M *et al.* An hypothesis concerning the space-time succession of *Calanus finmarchicus* in the northern North Sea. *ICES J Mar Sci* 1994;**51**:169–80. https://doi.org/10.1006/jmsc.1994.1018

Balazy K, Trudnowska E, Wojczulanis-Jakubas K *et al.* Molecular tools prove little auks from Svalbard are extremely selective for *Calanus glacialis* even when exposed to Atlantification. *Sci Rep* 2023;**13**:1–14. https://doi.org/10.1038/s41598-023-40131-7

Båmstedt U, Fosså JH, Martinussen MB *et al.* Mass occurrence of the physonect siphonophore *Apolemia uvaria* (Lesueur) in Norwegian waters. *Sarsia* 1998;**83**:79–85. https://doi.org/10.1080/00364827.1998.10413673

Beaugrand G. Monitoring pelagic ecosystems using plankton indicators. *ICES J Mar Sci* 2005;**62**:333–8. https://doi.org/10.1016/j.icesjms.2005.01.002

Beaugrand G, Brander KM, Lindley JA *et al.* Plankton effect on cod recruitment in the North Sea. *Nature* 2003;**426**:661–4. https://doi.org/10.1038/nature02164

Bosch-Belmar M, Milisenda G, Basso L *et al.* Jellyfish Impacts on Marine Aquaculture and Fisheries. *Rev Fish Sci Aquacult* 2020;**29**:242–59.

Brandão MC, Benedetti F, Martini S *et al.* Macroscale patterns of oceanic zooplankton composition and size structure. *Sci Rep* 2021;**11**:15714. https://doi.org/10.1038/s41598-021-94615-5

Buchner D, Leese F. BOLDigger—a python package to identify and organise sequences with the Barcode of Life Data systems. *Metabarcod Metagenom* 2020;**4**:e53535. https://doi.org/10.3897/mbmg.4.53535

Bucklin A, Kaartvedt S, Guarnieri M *et al.* Population genetics of drifting (*Calanus* spp.) and resident (*Acartia clausi*) plankton in Norwegian fjords. *J Plankton Res* 2000;**22**:1237–51. https://doi.org/10.1093/plankt/22.7.1237

Bucklin A, Lindeque PK, Rodriguez-Ezpeleta N *et al.* Metabarcoding of marine zooplankton: prospects, progress and pitfalls. *J Plankton Res* 2016;**38**:393–400. https://doi.org/10.1093/plankt/fbw023

Chen J, Chen MJ. Package 'GUniFrac.' The Comprehensive R Archive Network (CRAN). 2018. https://cran.r-project.org/web/packages/GUniFrac/index.html (1 April 2024, date last accessed).

Choquet M, Hatlebakk M, Dhanasiri AKS *et al.* Genetics redraws pelagic biogeography of Calanus. *Biol Lett* 2017;**13**:20170588. https://doi.org/10.1098/rsbl.2017.0588

Choquet M, Kosobokova KN, Kwaśniewski S *et al.* Can morphology reliably distinguish between the copepods *Calanus finmarchicus* and *C. glacialis*, or is DNA the only way? *Limnol Oceanogr: Methods* 2018;**16**:237–52. https://doi.org/10.1002/lom3.10240

Clarke A, Fraser KPP. Why does metabolism scale with temperature? *Funct Ecol* 2004;**18**:243–51. https://doi.org/10.1111/j.0269-8463.2004.00841.x

Coguiec E, Ershova EA, Daase M *et al.* Seasonal variability in the zooplankton community structure in a sub-Arctic fjord as revealed by morphological and molecular approaches. *Front Mar Sci* 2021;**8**:1–26. https://doi.org/10.3389/fmars.2021.705042

Coguiec E, Last KS, Cohen JH *et al.* Photoperiodism and overwintering in boreal and sub-Arctic *Calanus finmarchicus* populations. *Mar Ecol Prog Ser* 2023;**712**:49–65. https://doi.org/10.3354/meps14307

Culverhouse PF, Williams R, Reguera B *et al.* Do experts make mistakes? A comparison of human and machine identification of dinoflagellates. *Mar Ecol Prog Ser* 2003;**247**:17–25. https://doi.org/10.3354/meps247017

Drago L, Panaïotis T, Irisson JO *et al.* Global distribution of zooplankton biomass estimated by in situ imaging and machine learning. *Front Mar Sci* 2022;**9**:894372. https://doi.org/10.3389/fmars.2022.894372

Dugenne M, Corrales-Ugalde M, Luo J *et al.* First release of the pelagic size structure database: global datasets of marine size spectra obtained from plankton imaging devices. *Earth Syst Sci Data Disc* 2023;**2023**:1–41.

Ershova EA, Nyeggen MU, Yurikova DA *et al.* Seasonal dynamics and life histories of three sympatric species of *Pseudocalanus* in two Svalbard fjords. *J Plankton Res* 2021;**43**:209–23. https://doi.org/10.1093/plankt/fbab007

Ershova EA, Questel JM, Kosobokova KN *et al.* Population structure and production of four sibling species of *Pseudocalanus* spp. in the Chukchi Sea. *J Plankton Res* 2017;**39**:48–64. https://doi.org/10.1093/plankt/fbw078

Ershova EA, Wangensteen OS, Falkenhaug T. Mock samples resolve biases in diversity estimates and quantitative interpretation of zooplankton metabarcoding data. *Mar Biodivers* 2023;**53**:1–18. https://doi.org/10.1007/s12526-023-01372-x

Espinasse B, Basedow SL, Tverberg V *et al.* A major *Calanus finmarchicus* overwintering population inside a deep fjord in northern Norway: implications for cod larvae recruitment success. *J Plankton Res* 2016;**38**:604–9. https://doi.org/10.1093/plankt/fbw024

Evans LE, Hirst AG, Kratina P *et al.* Temperature-mediated changes in zooplankton body size: large scale temporal and spatial analysis. *Ecography* 2020;**43**:581–90. https://doi.org/10.1111/ecog.04631

Falkenhaug T. Distributional and seasonal patterns of ctenophores in Malangen, northern Norway. *Mar Ecol Prog Ser* 1996;**140**:59–70. https://doi.org/10.3354/meps140059

Falkenhaug T, Broms C, Bagøien E *et al.* Temporal variability of co-occurring *Calanus finmarchicus* and *C. helgolandicus* in Skagerrak. *Front Mar Sci* 2022;**9**:779335. https://doi.org/10.3389/fmars.2022.779335

Falkenhaug T, Nordby E, Svendsen H *et al.* Impact of advective processes on zooplankton biomass in a North Norwegian fjord system: a comparison between spring and autumn. In: HR Skjoldal, C Hopkins, KE Erikstad *et al.*(eds.), *Ecology of Fjords and Coastal Waters*. Amsterdam: Elsevier Science, 1995, 195–217.

Falkenhaug T, Tande KS, Semenova T. Diel, seasonal and ontogenetic variations in the vertical distributions of four marine copepods. *Mar Ecol Prog Ser* 1997;**149**:105–19. https://doi.org/10.3354/meps149105

Fleminger A, Hulsemann K. Geographical range and taxonomic divergence in North Atlantic Calanus (*C. helgolandicus*, *C. finmarchicus* and *C. glacialis*). *Mar Biol* 1977;**40**:233–48. https://doi.org/10.1007/BF00390879

Fosså JH. Mass occurrence of *Periphylla periphylla* (Scyphozoa, Coronatae) in a Norwegian fjord. *Sarsia* 1992;**77**:237–51. https://doi.org/10.1080/00364827.1992.10413509A

Gao S, Johnsen IA, Falkenhaug T *et al.* Particle exchange between coast and fjords and its biological implications. *Estuar Coast Shelf Sci* 2024;**299**:108689. https://doi.org/10.1016/j.ecss.2024.108689

García-Comas C, Sastri AR, Ye L *et al.* Prey size diversity hinders biomass trophic transfer and predator size diversity promotes it in planktonic communities. *Proc R Soc B* 2016;**283**:20152129, https://doi.org/10.1098/RSPB.2015.2129

Giering SLC, Culverhouse PF, Johns DG *et al.* Are plankton nets a thing of the past? An assessment of in situ imaging of zooplankton for large-scale ecosystem assessment and policy decision-making. *Front Mar Sci* 2022;**9**:986206.

Gorsky G, Flood PR, Youngbluth M *et al.* Zooplankton distribution in four western Norwegian fjords. *Estuar Coast Shelf Sci* 2000;**50**:129–35. https://doi.org/10.1006/ecss.1999.0540

Grosjean P, Denis K, Wacquet G. zooimage: analysis of numerical plankton images. 2018. https://cran.r-project.org/web/packages/zooimage/zooimage.pdf (1 April 2024, date last accessed).

R Harris, P Wiebe, J Lenz *et al.* (eds.), *ICES Zooplankton Methodology Manual*. San Diego: Elsevier, 2000

Hays GC, Richardson AJ, Robinson C. Climate change and marine plankton. *Trends Ecol Evol* 2005;**20**:337–44. https://doi.org/10.1016/j.tree.2005.03.004

Hopkins CCE. Ecological investigations on the zooplankton community of Balsfjorden, Northern Norway: changes in zooplankton abundance and biomass in relation of phytoplankton and hydrography, March 1976 - February 1977. In: G Rheinheimer *et al.* (ed.), *Lower Organisms and their Role in the Food Web: Proceedings of the 15th European Marine Biology Symposium, Kieler Meeresforschungen*. Sonderheft, 5, 1981, 124–139.

Hopkins CCE, Tande KS, Grønvik S *et al.* Ecological investigations of the zooplankton community of Balsfjorden, Northern Norway: an analysis of growth and overwintering tactics in relation to niche and environment in *Metridia longa* (Lubbock), *Calanus finmarchicus* (Gunnerus), *Thysanoessa inermis* (Krøyer) and T. raschi (M. Sars). *J Exp Mar Biol Ecol* 1984;**82**:77–99.

Horne CR, Hirst AG, Atkinson D *et al.* A global synthesis of seasonal temperature–size responses in copepods. *Global Ecol Biogeogr* 2016;**25**:988–99. https://doi.org/10.1111/geb.12460

Hosia A. Gelatinous zooplankton in western Norwegian fjords. Ecology, systematics and comparisons with adjacent waters. *Mar Biol* 2007;**151**:177–84, https://doi.org/10.1007/S00227-006-0466-2

Hosia A, Båmstedt U. Seasonal abundance and vertical distribution of siphonophores in western Norwegian fjords. *J Plankton Res* 2008;**30**:951–62. https://doi.org/10.1093/plankt/fbn045

Inall ME, Gillibrand PA. The physics of mid-latitude fjords: A review. *Geol Soc London Spec Publ* 2010;**344**:17–33. https://doi.org/10.1144/SP344.3

Jøssang I. The energy budget of a local jellyfish proliferation: *Periphylla periphylla* in the Trondheimsfjord, Norway. NTNU, Trondheim, Norway, 2015. https://ntnuopen.ntnu.no/ntnu-xmlui/handle/11250/2358864.

Knutsen T, Hosia A, Falkenhaug T *et al.* Coincident mass occurrence of gelatinous zooplankton in Northern Norway. *Front Mar Sci* 2018;**5**:290509. https://doi.org/10.3389/fmars.2018.00158

Marlétaz F, Le Parco Y, Liu S *et al.* Extreme mitogenomic variation in natural populations of chaetognaths. *Genome Biol Evolut* 2017;**9**:1374–84. https://doi.org/10.1093/gbe/evx090

Melle W, Runge J, Head E *et al.* The North Atlantic Ocean as habitat for *Calanus finmarchicus*: environmental factors and life history traits. *Prog Oceanogr* 2014;**129**:244–84. https://doi.org/10.1016/j.pocean.2014.04.026

Michelsen HK, Svensen C, Reigstad M *et al.* Seasonal dynamics of meroplankton in a high-latitude fjord. *J Mar Syst* 2017;**168**:17–30. https://doi.org/10.1016/j.jmarsys.2016.12.001

Moriarty R, Buitenhuis ET, Le Quéré C. Distribution of known macrozooplankton abundance and biomass in the global ocean. *Earth Syst Sci Data* 2013;**5**:241–57. https://doi.org/10.5194/essd-5-241-2013

Motoda S. Devices of simple plankton apparatus. *Mem Fac Fish Hokkaido Univ* 1959;**7**:73–94.

O'Brien TD, Blanco-Bercial L, Questel JM *et al.* MetaZooGene Atlas and Database: reference sequences for marine ecosystems. *Methods Mol Biol* 2024;**2744**:475–89. https://doi.org/10.1007/978-1-0716-3581-0_28

Oksanen J, Kindt R, Pierre L *et al.* vegan: community ecology package, R package version 2.4-0. R package version. 2016, 22–1. https://cran.r-project.org/web/packages/vegan/index.html (1 April 2024, date last accessed).

Polyakov IV, Alkire MB, Bluhm BA *et al.* Borealization of the Arctic Ocean in response to anomalous advection from sub-Arctic seas. *Front Mar Sci* 2020;**7**:1–32. https://doi.org/10.3389/fmars.2020.00491

R Core Team. *R: A Language and Environment for Statistical Computing*. 2022. https://www.R-project.org.

Ratnarajah L, Abu-Alhaija R, Atkinson A *et al.* Monitoring and modelling marine zooplankton in a changing climate. *Nat Commun* 2023;**14**:1–17. https://doi.org/10.1038/s41467-023-36241-5

Renaud PE, Daase M, Banas NS *et al.* Pelagic food-webs in a changing Arctic: a trait-based perspective suggests a mode of resilience. *ICES J Mar Sci* 2018;**75**:1871–81. https://doi.org/10.1093/icesjms/fsy063

Richardson AJ. In hot water: zooplankton and climate change. *ICES J Mar Sci* 2008;**65**:279–95. https://doi.org/10.1093/icesjms/fsn028

R Sætre. *The Norwegian Coastal Current : Oceanography and Climate*. Trondheim, Norway: Tapir Academic Press, 2007, 159.

Samuelsen A, Huse G, Hansen C. Shelf recruitment of *Calanus finmarchicus* off the west coast of Norway: role of physical processes and timing of diapause termination. *Mar Ecol Prog Ser* 2009;**386**:163–80. https://doi.org/10.3354/meps08060

Skaala Ø, Sjøtun K, Dahl E *et al.* Interactions between salmon farming and the ecosystem: lessons from the Hardangerfjord, western Norway. *Mar Biol Res* 2014;**10**:199–202. https://doi.org/10.1080/17451000.2013.840730

Skjoldal HR. Species composition of three size fractions of zooplankton used in routine monitoring of the Barents Sea ecosystem. *J Plankton Res* 2021;**43**:762–72. https://doi.org/10.1093/plankt/fbab056

Skjøldal HR, Hopkins C, Erikstad KE *et al. Ecology of Fjords and Coastal Waters*. Amsterdam: Elsevier, 1995

Skjøldal HR, Wiebe PH, Postel L *et al.* Intercomparison of zooplankton (net) sampling systems: results from the ICES/GLOBEC sea-going workshop. *Prog Oceanogr* 2013;**108**:1–42. https://doi.org/10.1016/j.pocean.2012.10.006

Somme JD. Animal plankton of the Norwegian coast waters and the open sea I. Production of *Calanus finmarchicus* (Gunner) and *Calanus hyperboreus* (Kroyer) in the Lofoten area. *Fisk dir skr Ser Havunders* 1934;**4**:1–163.

Sørnes TA, Aksnes DL, Båmstedt U *et al.* Causes for mass occurrences of the jellyfish *Periphylla periphylla*: a hypothesis that involves optically conditioned retention. *J Plankton Res* 2007;**29**:157–67. https://doi.org/10.1093/plankt/fbm003

Sprules WG, Barth LE. Surfing the biomass size spectrum: some remarks on history, theory, and application. *Can J Fish Aquat Sci* 2016;**73**:477–95. https://doi.org/10.1139/cjfas-2015-0115

JH Steeleed. *Spatial Pattern in Plankton Communities*. New York, NY: Springer US, 1978.

Steinberg DK, Landry MR. Zooplankton and the Ocean Carbon Cycle. *Annu Rev Mar Sci* 2017;**9**:413–44. https://doi.org/10.1146/annurev-marine-010814-015924

Strømgren T. Zooplankton diversity in four Norwegian fjords. *Sarsia* 1975;**59**:15–30. https://doi.org/10.1080/00364827.1975.10411284

Sutor M, Cowles TJ, Peterson WT *et al.* Comparison of acoustic and net sampling systems to determine patterns in zooplankton distribution. *J Geophys Res: Oceans* 2005;**110**:1–11. https://doi.org/10.1029/2004JC002681

Vihtakari M. ggOceanMaps: Plot Data on Oceanographic Maps using "ggplot2. 2024.https://mikkovihtakari.github.io/ggOceanMaps/ (1 April 2024, date last accessed).

Weatherdon LV, Magnan AK, Rogers AD *et al.* Observed and projected impacts of climate change on marine fisheries, aquaculture, coastal tourism, and human health: an update. *Front Mar Sci* 2016;**3**:179990. https://doi.org/10.3389/fmars.2016.00048

Weydmann A, Walczowski W, Carstensen J *et al.* Warming of Subarctic waters accelerates development of a key marine zooplankton *Calanus finmarchicus*. *Global Change Biol* 2018;**24**:172–83. https://doi.org/10.1111/gcb.13864

Wiborg KF. Zooplankton in relation to hydrography in the Norwegian Sea. *Fisk dir skr Ser Havunders* 1955;**11**:1–66.

Wiebe PH, Benfield MC. From the Hensen net toward four-dimensional biological oceanography. *Prog Oceanogr* 2003;**56**:7–136. https://doi.org/10.1016/S0079-6611(02)00140-4

Wood SN. Fast stable restricted maximum likelihood and marginal likelihood estimation of semiparametric generalized linear models. *J R Stat Soc Ser B* 2011;**73**:3–36. https://doi.org/10.1111/j.1467-9868.2010.00749.x

Zhou M. What determines the slope of a plankton biomass spectrum? *J Plankton Res* 2006;**28**:437–48. https://doi.org/10.1093/plankt/fbi119

Handling Editor: Rubao Ji